Photooxidation of Amino Acids and Proteins Mediated by Novel 1,8-Naphthalimide Derivatives

Bindu Abraham and Lisa A. Kelly*

Department of Chemistry and Biochemistry, University of Maryland, Baltimore County, 1000 Hilltop Circle, Baltimore, Maryland 21250

Received: June 26, 2003; In Final Form: September 3, 2003

The ground- and excited-state interactions of *N*-(2-ethanoic acid)-1,8-naphthalimide (NI-ala), along with tryptophan and tyrosine-substituted 1,8-naphthalimide derivatives (NI-trp and NI-tyr), with amino acids and native proteins have been studied in aqueous buffered solution. The singlet excited state of NI-ala reacts with the aromatic amino acids, tryptophan, tyrosine, and histidine with a rate constant at or exceeding the diffusion-controlled limit. Reactivity with bovine serum albumin (BSA) and lysozyme was also demonstrated. However, in all cases, no long-lived redox products were observed from the singlet state quenching. The reactivity of the triplet excited state of NI-ala with the individual amino acids and proteins was studied using laser flash photolysis. Triplet-state reactivity was demonstrated with tryptophan and tyrosine, along with BSA and lysozyme proteins. In the case of tryptophan, tyrosine, and lysozyme, long-lived redox products were observed and quantified. Neutral tryptophan and tyrosyl radicals were observed by transient spectroscopy as quenching products. Upon photolysis of all three 1,8-naphthalimide derivatives, both cleavage and cross-linking of the lysozyme are observed. These studies have identified the potential oxidative targets in native proteins and demonstrated the utility of our naphthalimide derivatives to photomodify native proteins.

Introduction

Biomolecular interactions, particularly those involving nucleic acids and proteins with each other or with small molecules, are ubiquitous and critical to maintaining structure and function. Information obtained from conventional spectroscopies (vibrational, circular dichroism, NMR) and X-ray diffraction techniques is limited by the abilities to resolve individual transitions and crystallize the complex. As an alternative method of probing these interactions, site-selective cleavage or cross-linking of peptides and proteins has become an important method in molecular biology to elucidate protein structure and molecular interactions. Proteolytic enzymes have been traditionally used, but their activity is limited to particular pH and temperature ranges as well as solvent. Chemical reagents, such as cyanogen bromide[1] and *N*-bromosuccinimide,[2] have been shown to induce selective cleavage at methionine and tryptophan residues, respectively. However, these reagents generally require harsh conditions that may result in nonselective protein degradation.

Under milder conditions, transition-metal complexes have been developed to activate amide bond hydrolysis. For example, palladium(II) and platinum(II) complexes have been recently shown to site selectively hydrolyze tryptophan-containing peptides by coordinating to the indole residue and adjacent amide group.[3,4]

The development of synthetic, photoactive compounds capable of site-selective protein cleavage offers an alternative approach to thermal chemistry. Photoactivated probes are attractive alternatives to thermally activated compounds, since the reaction can be turned on and off on demand, allowing the structure-probing reaction to be timed with respect to macromolecule dynamics. In a series of papers, protein photocleavage has been demonstrated using pyrenyl peptide derivatives.[5−8] The probes were shown to noncovalently associate with bovine serum albumin (BSA) and lysozyme. When the pyrene was electronically excited in the presence of an electron acceptor, site-selective cleavage was observed following reaction of the protein with the deprotonated pyrene radical cation. Despite its utility, reports of new photoactive probes of protein structure have been surprisingly absent.

At the same time, the specific contact points in multiprotein complexes can be probed using reagents that are capable of inducing protein−protein cross-links. Although reactive intermediates have been developed as photoaffinity reagents capable of nonspecific attack (e.g., by hydrogen atom abstraction from the C_α carbon), residue-specific tools must be developed to probe specific points of contact. Electron-rich aromatic amino acids, such as tryptophan and tyrosine, are viable targets for site-specific oxidative damage. In recent reports, tyrosine has been implicated as a key residue in the oxidative cross-linking of proteins.[9−12]

In a separate report, dityrosine was shown to be formed upon the flavin-mediated photooxidation of a water-soluble, tyrosine-containing polymer.[13] Photochemical cross-linking was also demonstrated using long wavelength absorbing porphyrin and tris(bipyridyl)ruthenium(II) probes.[14,15]

Within proteins, tyrosine and tryptophan residues have been shown to be the location of stable radical trap sites.[16−18] Formation of these radical traps has found utility in developing novel structural probes. For example, DNA−peptide adducts were shown to be formed following the photoinduced oxidation of guanine in a DNA−peptide complex.[19] A DNA-bound tyrosyl radical was shown to form an adduct with DNA, selectively cross-linking to the AT binding site.

Naphthalenimides represent a class of molecules that have been shown to demonstrate a diversity of reactivity toward

* To whom correspondence should be addressed: e-mail LKelly@umbc.edu.

10.1021/jp0358275 CCC: $25.00
Published on Web 10/21/2003

biological substrates, including DNA and proteins. In their ground state, 1,8-naphthalimide derivatives have been shown to have antitumor potential.[20−23] When electronically excited with long wavelength UV light, certain of these compounds have been shown to have utility as "photo-Fenton"[24] and guanine-specific cleavage agents.[25,26] The mechanism of damage has been shown to depend on naphthalimide structure and reaction conditions (presence of dissolved oxygen and naphthalimide concentration).[27,28]

In separate reports, naphthalimide derivatives have been shown to have utility as protein/peptide structural probes. 4-(Alkylamino)-1,8-naphthalimides have been shown to photo-induce the cross-linking in RNase.[29] Hydroperoxynaphthalimide derivatives were also found to bind to the heme pocket of horseradish peroxidase. Upon photoexcitation, peptide chain cleavage was observed. The heme group was destroyed, and the formation of *N*-formylkynurenine following tryptophan oxidation was attributed to the photochemical formation of hydroxyl radical.[30]

In this paper, we report the synthesis and characterization of three novel, water-soluble 1,8-naphthalimide compounds. The ground- and excited-state interactions of these compounds with amino acids and native proteins have been characterized to elucidate the mechanisms and targets for oxidative damage. Preliminary results are also reported that demonstrate the utility of these compounds as structural probes capable of both cleaving and cross-linking native proteins.

Experimental Section

Materials. Tyrosine (99%) was obtained from Fluka and used as received. Tryptophan (98%) was obtained from Sigma and recrystallized from methanol prior to use. Cysteine (98%), alanine (99+%), and histidine (99+%) were obtained from Aldrich as the L-isomers. Cysteine was recrystallized (1×) from water prior to use, while alanine and histidine were used as received. Sodium hydrogen phosphate (99%) was obtained from Aldrich and used as received. 1,8-Naphthalic anhydride (97%, Acros) was recrystallized two times from DMF and dried in vacuo prior to use. *N*-(2-Ethanoic acid)-1,8-naphthalimide (NI-ala) was prepared by the reaction of β-alanine (99%, Aldrich) and commercially available 1,8-naphthalic anhydride as previously described.[31] Sodium dodecyl sulfate (SDS, 99%) was obtained from Pharmacia Biotech, and the acrylamide solution was obtained from Bio-Rad Laboratories as a 30% acrylamide:bis(acrylamide) (29:1) solution. Other materials and solvents were obtained from commercial sources.

Bovine serum albumin (BSA; MW 66 267) and lysozyme (MW 14 300) were obtained from Aldrich and USB Corp., respectively. Protein stock solutions were prepared by dissolving the solid in 0.01 M pH 7.00 sodium phosphate buffer (PB). The concentration of each solution was determined by using extinction coefficients at 280 nm for BSA and lysozyme of 43 291 and 37 646 M^{-1} cm^{-1}, respectively.[32]

***N*-(4-Hydroxyphenylpropionic acid)-1,8-naphthalenimide (NI-tyr)** was prepared by adding a 1:1 molar ratio of 1,8-naphthalic anhydride (2.73 g) and L-tyrosine (2.37 g) to 80 mL of DMF. The mixture was heated at 120 °C for 3.5 h. Thin-layer chromatography was done to confirm product formation. The solvent was rotary evaporated under vacuum, and the resultant solid was isolated. The formation of the compound was confirmed using thin-layer chromatography and NMR. The compound was recrystallized from methanol (3×), and the purity of the compound was assessed by elemental analysis. ϵ (344 nm; pH 7.0 phosphate buffer) = 12 820 ± 150 M^{-1} cm^{-1}. ^{1}H NMR (DMSO-d_6): 8.54 (dd, 4H, napht), 7.95 (dd, 2H, napht), 6.85 (d, 2H phen), 6.45 (d, 2H phen), 5.80 (t, 1H, CH), 3.40 (m, 2H, CH_2) 13.00 (broad, 1H, −COOH) Anal. Calcd: C, 69.80; H, 4.18; N, 3.88. Found: C, 69.70; H, 4.18; N, 3.88.

***N*-((Indolyl)propionic acid))-1,8-naphthalenimide (NI-trp)** was prepared by adding a 1:1 molar ratio of 1,8-naphthalic anhydride (2.06 g) and L-tryptophan (2.26 g) to 50 mL of DMF. The mixture was heated at 120 °C for 4 h. Thin-layer chromatography was done to confirm product formation. The solvent was rotovaped, and the resultant solid was isolated. The formation of the compound was confirmed using thin-layer chromatography and NMR. The compound was recrystallized in acetonitrile (3×), and the purity of the compound was assessed by elemental analysis. ϵ (344 nm; pH 7 phosphate buffer) = 14 300 ± 200 M^{-1} cm^{-1}. ^{1}H NMR (DMSO-d_6): 8.54 (dd, 4H, napht), 7.80 (dd, 2H, napht), 7.50 (d, 1H indole), 7.20 (d, 1H indole), 7.10 (s, 1H, indole), 6.95 (t, 1H, indole), 6.80 (t, 1H, indole) 5.80 (t, 1H, CH), 3.60 (m, 2H, CH_2), 10.80 (s, 1H, NH), 13.00 (broad, 1H, −COOH) Anal. Calcd: C, 71.87; H, 4.20; N, 7.29. Found: C, 71.69; H, 4.16; N, 7.26.

General Techniques. Ground-state UV/vis absorption spectra were recorded with a JASCO V-570 double-beam spectrometer. Fluorescence spectra were measured using a SPEX Fluoromax-2 fluorescence spectrometer. Fluorescence quantum yields were measured using 1,8-naphthalimide in a pH 7.0 buffered aqueous solution as a standard with a known ϕ_f of 0.44.[27] An excitation wavelength of 344 nm was used. All solutions were air-saturated. Nanosecond transient absorption studies were carried out using the technique of laser flash photolysis. Pulsed excitation at 355 nm was provided by the third harmonic of a Q-switched Nd:YAG laser. The system has been previously described.[33] All solutions were argon-purged unless otherwise indicated.

To obtain the concentration of excited states produced, a pair of optically matched solutions containing an aqueous solution of naphthalimide or acetonitrile solution of benzophenone was subjected to identical flash intensity. Plots of the ΔA_{520} and ΔA_{480}, as a function of laser intensity, were constructed. From a ratio of the slopes, along with the known T_1-T_n extinction coefficient of benzophenone (6500 M^{-1} cm^{-1} at 520 nm),[34] the concentration of naphthalimide excited states was determined and used to evaluate the quantum efficiencies of charge separation.

Steady-state photolyses were carried out using a 450 W mercury vapor lamp (Ace Glass, Vineland, NJ). The samples were photolyzed in a turntable reactor maintained at 25 °C during photolysis. Filters (Schott WG320) were placed between the lamp and samples to prevent direct irradiation of the protein samples. Samples were irradiated in Pyrex glass tubes, and aliquots were removed at hourly intervals.

Results

Ground-State Interactions of Naphthalimides (NI's) with BSA and Lysozyme. The structures of the naphthalimide derivatives used in this study are shown in Figure 1. The compounds possess an aromatic naphthalimide moiety, along with anionic side chains. Phenylic moieties have been previously reported to associate with BSA and lysozyme,[5,7] and the negatively charged side group should facilitate binding to positively charged domains in the native proteins, if available. To assess ground-state interactions of these compounds with the proteins employed, UV/vis spectroscopy was used. Upon addition of BSA or lysozyme (up to 150 μM) to a buffered

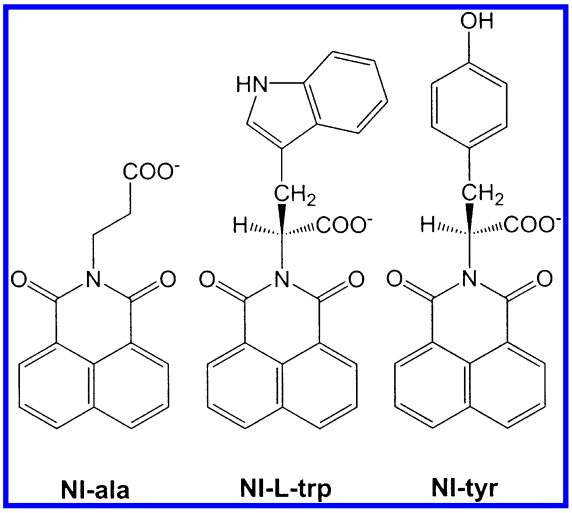

Figure 1. Structure of 1,8-naphthalimide derivatives used in this work.

solution of NI-ala, NI-tyr, or NI-trp, no spectral changes were observed in the regions above 300 nm, where the absorbance of the protein is negligible. Using a combination of fluorescence spectroscopy and laser flash photolysis, the reactivities of NI excited states with amino acids and native proteins were elucidated.

Singlet-State Quenching by Amino Acids and Proteins. To study the interactions of the excited singlet state of NI with native proteins and the individual amino acids, a combination of fluorescence and transient absorption spectroscopies was employed. The fluorescence quantum yields of each of the three 1,8-naphthalimide derivatives shown in Figure 1 were measured in 10 mM phosphate buffer (pH 7.00). The quantum yield of NI-ala was determined to be 0.339 ± 0.021, very similar to that previously reported for the parent 1,8-naphthalimide chromophore in aqueous buffered solvent.[27,35] The fluorescence quantum yields of NI-trp (ϕ_f = 0.0046 ± 0.0007) and NI-tyr (ϕ_f = 0.0021 ± 0.0003) were ca. 100 times lower than that measured for NI-ala. We attribute the diminished fluorescence to competitive intramolecular electron transfer in the -trp and -tyr linked derivatives.

The ability of each of the amino acids and two native proteins to react with the singlet excited state of NI-ala was assessed using steady-state fluorescence spectroscopy. The results are shown in Figure 2. As seen in Figure 2a, the addition of tryptophan to a pH 7.0 phosphate buffered solution of NI-ala resulted in quenching of the fluorescence. Quenching is also observed using BSA (Figure 2b). For both the individual amino acid and native protein, no shifts in the fluorescence spectra are observed.

The fluorescence quenching data shown in Figure 2, along with data from other amino acids and lysozyme, were fitted to a Stern−Volmer bimolecular quenching model (eq 1).

$$I_0/I = 1 + k_{S_1}\tau_{S_1}[Q] \qquad (1)$$

In eq 1, I_0 and I are the fluorescence intensities in the absence and presence of amino acid or protein quencher (Q), respectively, k_{S_1} is the bimolecular rate constant for quenching of ^{1}NI-ala* by each quencher, and τ_{S_1} is the lifetime of ^{1}NI-ala*. Stern−Volmer plots for quenching by amino acids and proteins are shown in the insets of Figure 2, a and b, respectively. In all cases, linear Stern−Volmer plots are obtained. A singlet-state lifetime of 2.6 ns was determined using picosecond pump−probe spectroscopy,[36] monitoring the decay kinetics of the S_1−S_n transition at 440 nm. From the slopes of the plots shown in

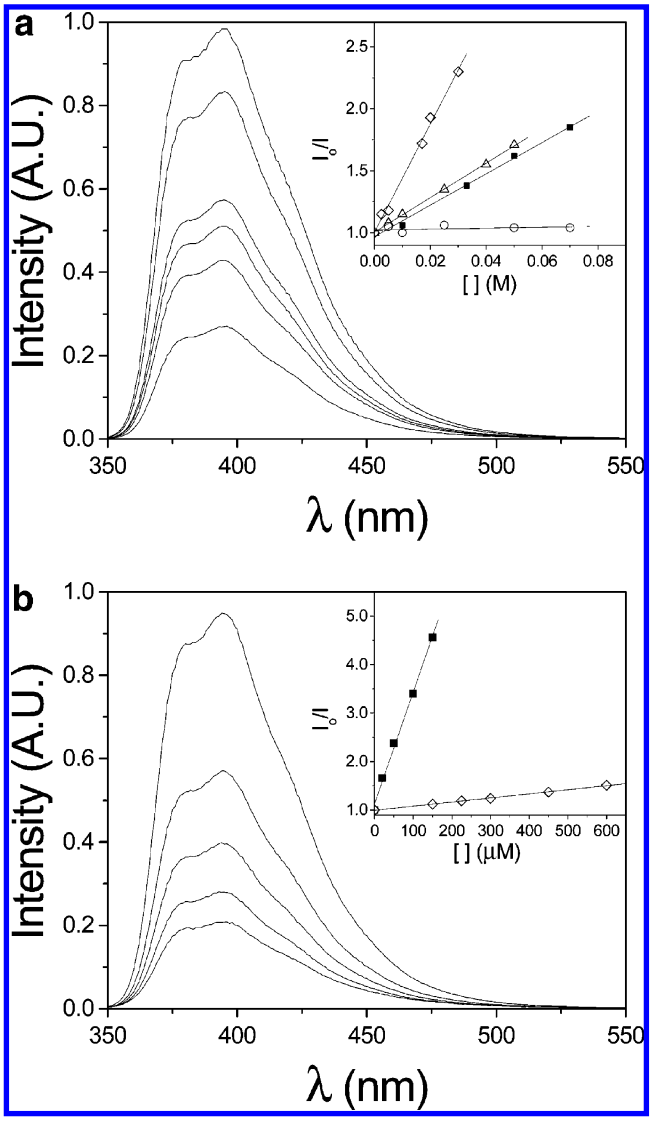

Figure 2. Fluorescence spectra of a pH 7.0 phosphate buffered solution containing 10 μM NI-ala and (a) 0, 5, 17, 20, 30, and 40 mM tryptophan (top to bottom spectra); (b) 0, 20, 50, 100, and 150 μM BSA (top to bottom spectra). Insets show Stern−Volmer plots for quenching of ^{1}NI-ala* by (a) tryptophan (diamonds), histidine (triangles), tyrosine (squares), and alanine (circles) and (b) BSA (squares) and lysozyme (diamonds) (λ_{ex} = 344 nm).

Figure 2, along with the singlet-state lifetime, bimolecular rate constants for the quenching of ^{1}NI-ala* by the amino acids, BSA, and lysozyme were obtained. Of the amino acids, measurable quenching was observed only with the aromatic amino acids tryptophan, tyrosine, and histidine. No quenching was observed for nonaromatic amino acids, such as alanine or lysine. The bimolecular rate constants are summarized in Table 1. Because of the short singlet-state lifetime of NI-tyr and NI-trp, diffusional quenching by amino acids or proteins is not observed at the amino acid concentrations used.

Naphthalimide Triplet-State Quenching by Amino Acids and Proteins. The T_1−T_n absorption spectra of 1,8-naphthalimide (NI) derivatives have been published.[28,27] The spectrum of NI possesses an absorption maximum at 480 nm, independent of the substituent on the imide nitrogen. For NI-ala, the triplet-state lifetime in argon-saturated, dilute aqueous solution (6 μM NI in 10 mM pH 7.0 phosphate buffer) was measured to be 120 μs. Upon addition of tryptophan or tyrosine, the triplet-state decay kinetics are modified. As shown in Figure 3a, a new absorption band at 400 nm is observed with increasing

TABLE 1: Summary of Bimolecular Quenching Constants and Radical Yields for the Quenching of the Singlet and Triplet Excited State of NI-ala by Amino Acids and Proteins

amino acid or protein	k_{S_1} ($\times 10^{-9}$ M^{-1} s^{-1})[a]	k_{T_1} ($\times 10^{-9}$ M^{-1} s^{-1})[b]	$\phi_{NI^{\bullet -}}$ [b]
tryptophan	16.0 ± 0.8	2.60 ± 0.16	0.52 ± 0.04
tyrosine	5.27 ± 0.86	0.89 ± 0.03	0.33 ± 0.05
histidine	5.03 ± 0.16	<0.001	
BSA	8360 ± 170	0.46 ± 0.02	
lysozyme	325 ± 8	0.76 ± 0.01	0.23 ± 0.02

[a] [NI-ala] = 10 μM in 10 mM pH 7.0 phosphate buffer. [b] Radical production efficiency from triplet-state quenching only. [NI-ala] = 10 μM in 10 mM pH 7.0 phosphate buffer.

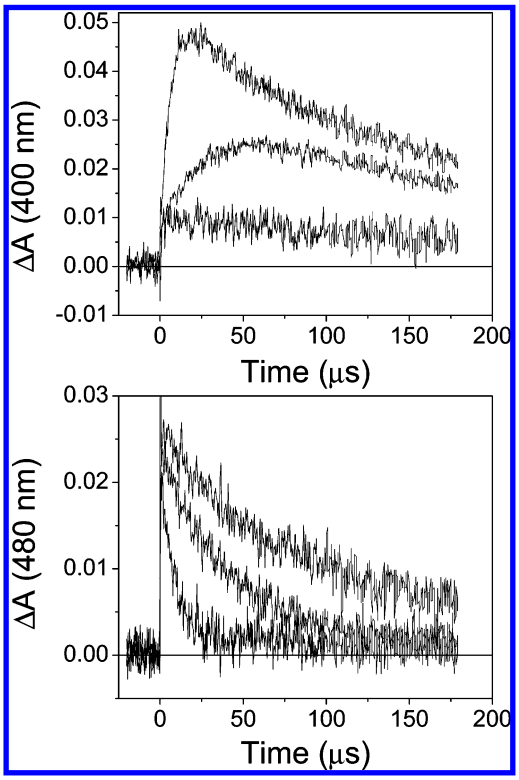

Figure 3. Pseudo-first-order decay of ^{3}NI-ala* monitored at 480 nm (10 μM in 10 mM pH 7.0 phosphate buffer) in the presence of 0, 20, and 160 μM (bottom panel) tyrosine. Top panel shows concomitant formation of $NI^{\bullet -}$ in the presence of 0, 20, and 160 μM tyrosine. All solutions are deoxygenated.

concentrations of tyrosine. Simultaneously, the rate constant for triplet decay increases (Figure 3b) and is concomitant with the growth of the 400 nm transient. Significant quenching by other amino acids, including histidine and lysine, was not observed. The transient absorption spectrum of the triplet-state quenching product formed from either tyrosine or tryptophan is identical to the one-electron-reduced form of NI-ala.[37] No measurable transients were observed upon laser flash excitation of NI-trp or NI-tyr, suggesting that rapid intramolecular electron transfer is followed by charge recombination within the pulse duration. Diffusional production of the one-electron-reduced naphthalimide is shown in eq 2b, where Q is the amino acid quencher.

$$^3NI^* \rightarrow NI \qquad (2a)$$

$$^3NI^* + Q \rightarrow NI^{\bullet -} + Q^{\bullet +} \qquad k_{T_1} \qquad (2b)$$

To investigate the possibility of triplet-mediated amino acid oxidation in native proteins, BSA and lysozyme were used as triplet-state quenchers. As shown in Figure 4, addition of

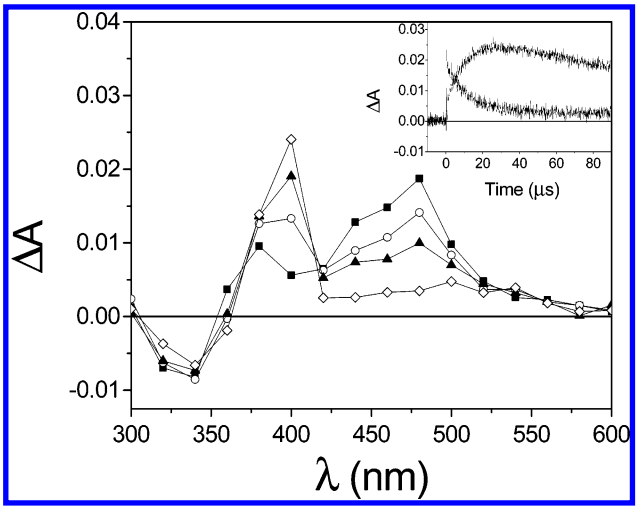

Figure 4. Transient absorption spectra showing production of $NI^{\bullet -}$ following quenching of ^{3}NI-ala* by lysozyme (NI-ala and lysozyme concentrations are 10 and 75 μM, respectively, in argon-saturated pH 7.0 phosphate buffer (10 mM)). Spectra shown are 1 μs (squares), 5 μs (circles), 10 μs (triangles), and 30 μs (diamonds) after 355 nm excitation. Inset: concomitant growth of $NI^{\bullet -}$ at 400 nm and triplet decay at 480 nm.

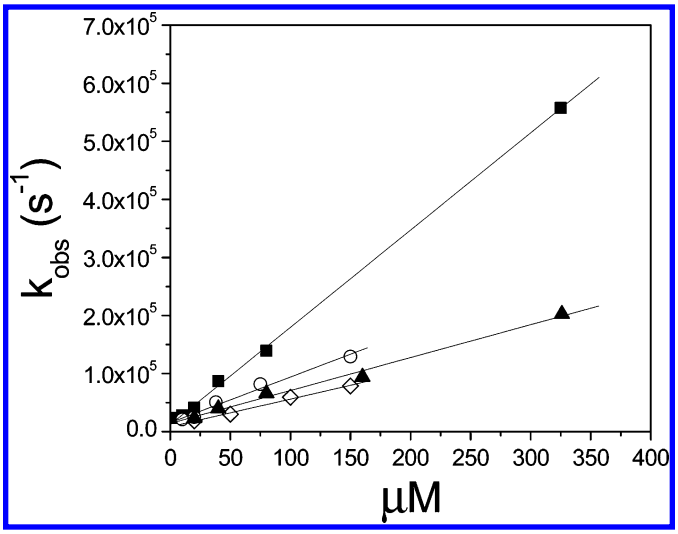

Figure 5. Bimolecular quenching plot (eq 2) for quenching of ^{3}NI-ala* by amino acids (trp (squares), tyr (triangles), BSA (diamonds), and lys (circles)). [NI] = 10 μM in deoxygenated buffer solution (10 mM phosphate buffer, pH 7.0).

lysozyme to a phosphate buffered solution of NI-ala resulted in quenching of the T_1-T_n absorption at 480 nm. Concomitant growth of the NI-ala radical anion at 400 nm is clearly observed. Similarly, BSA was also found to quench the triplet excited state. However, the NI-ala radical anion was not observed, even under conditions where the triplet state was completely quenched. By analogy to our amino acid results, we attribute the triplet-state quenching (and radical anion production observed using lysozyme as the quencher) to electron transfer from oxidizable residues (tyrosine and tryptophan) in the native protein.

Bimolecular quenching plots for the quenching of ^{3}NI-ala* by amino acids and native proteins are shown in Figure 5. In all cases, linear quenching plots were obtained. The bimolecular rate constants, k_{T_1}, were obtained from the slopes of these plots. The rate constants are summarized in Table 1.

Quantum Efficiency of Radical Formation. Having characterized the kinetics of triplet reactivity with amino acids and proteins, the yields of charge-separated products (ϕ_{ce}) were determined. The quantum yield of NI-ala radical anion produced

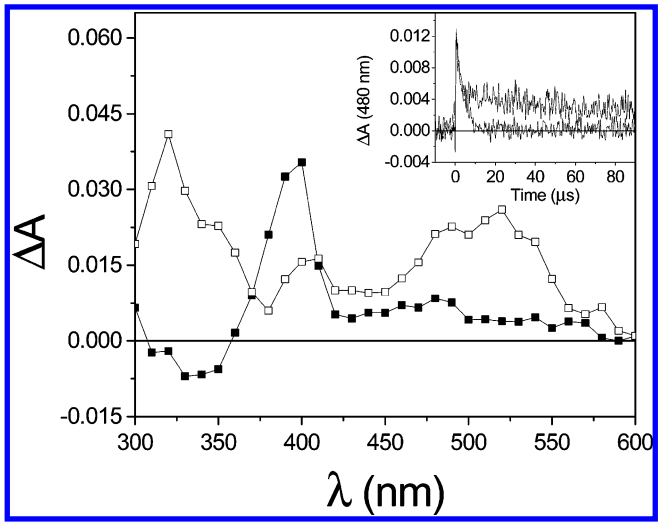

Figure 6. Transient absorption spectra of an air-saturated aqueous solution containing 10 μM NI-ala and 1.045 mM tryptophan. Spectra are recorded 1.2 μs (solid squares) and 20 μs (open squares) after 355 nm excitation (20 μs spectrum has been multiplied by a factor of 5). Decay traces recorded at 480 nm are shown in the inset for a solution containing 1.045 mM tryptophan (top trace) and 0 mM tryptophan (bottom trace).

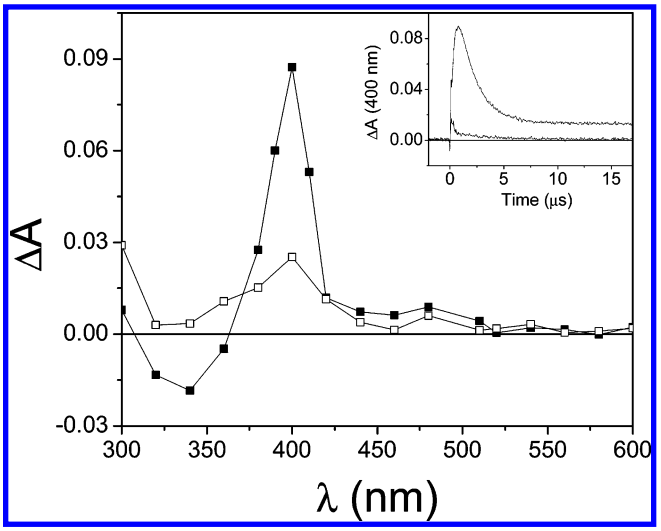

Figure 7. Transient absorption spectra of an air-saturated aqueous solution containing 10 μM NI-ala and 2.245 mM tryptophan. Spectra are recorded 0.9 μs (solid squares) and 15 μs (open squares) after 355 nm excitation (15 μs spectrum has been multiplied by a factor of 2). Decay traces recorded at 400 nm are shown in the inset for a solution containing 2.245 mM tryptophan (top trace) and 0 mM tryptophan (bottom trace).

from the triplet-mediated amino acid oxidation was evaluated from eq 3.

$$\frac{\Delta A_{\mathrm{NI}^{\bullet-}}}{[\mathrm{NI}^*]_0} = \Delta\epsilon_{\mathrm{NI}^{\bullet-}} f_q \phi_{ce} \qquad (3)$$

In eq 3, $\Delta A_{\mathrm{NI}^{\bullet-}}$ is the transient absorbance from the one-electron-reduced naphthalimide (obtained by extrapolating the decay component to time zero), $[\mathrm{NI}^*]_0$ is the concentration of NI excited states determined using a solution of benzophenone as an actinometer, $\Delta\epsilon_{\mathrm{NI}^{\bullet-}}$ is the extinction coefficient of the radical ($\Delta\epsilon_{\mathrm{NI}^{\bullet-}} = 29\,000\ \mathrm{M}^{-1}\ \mathrm{cm}^{-1}$),[28] and f_q is the fraction of triplet states quenched by the amino acid or protein. Quantum yields of radical production following tryptophan, tyrosine, or lysozyme quenching were determined from plots of the laser-induced absorption change at 400 nm ($\Delta A_{\mathrm{NI}^{\bullet-}}$), normalized to the initial concentration of NI excited states ($[\mathrm{NI}^*]_0$), as a function of f_q. From plots to eq 3, the quantum efficiencies of radical production were determined and are summarized in Table 1. In evaluating these quantum efficiencies, we have assumed that the contribution to the transient absorption signal at 400 nm from the oxidized amino acid is negligible.

The spectra of both tyrosine and tryptophan radicals are published.[19,38]Although the tyrosyl radical spectrum possesses an absorption maximum at 400 nm, the extinction coefficient is more than an order of magnitude smaller ($\epsilon = 2000\ \mathrm{M}^{-1}\ \mathrm{cm}^{-1}$)[39] than that of the NI-ala radical anion. In the case of tryptophan, the absorption of the radical at 400 nm is substantially smaller.[40] Thus, we assume that the contribution of these absorbances is negligible for the sake of quantifying NI-ala radical anion production.

Observation of Oxidized Amino Acids. Finally, to strengthen the hypothesis that tyrosine and tryptophan radicals are being formed, transient absorption spectra of an air-saturated solution containing NI-ala and each amino acid were recorded. A sufficiently high concentration of the amino acid was added to quench >95% of the triplet excited states in the air-saturated solutions. In the presence of dissolved oxygen, the NI-ala radical anion is scavenged by molecular oxygen with a diffusion-controlled rate constant, allowing the absorption spectrum of the remaining product to be observed. Shown in Figure 6 are the results of this experiment using tryptophan quencher. At early times (ca. 1 μs after the pulse), the spectrum shows the predominant NI-ala$^{\bullet-}$ absorption at 400 nm. At longer times (>20 μs), the absorbance of this species disappears due to quenching by dissolved oxygen (see bottom kinetic trace in the inset of Figure 6). The transient absorption spectrum of the remaining species shows features at ca. 520 and 320 nm. These spectral features are identical to those of the tryptophan radical produced following one-electron oxidation of the amino acid.[19,41] The identical experiment was carried out using tyrosine as the quencher. The results are shown in Figure 7. As shown in the inset of Figure 7, growth of the NI-ala radical anion is observed within 1−2 μs after the pulse. At longer times, the absorbance decays with first-order kinetics to a residual, long-lived transient. The spectrum of this transient (open squares in Figure 7) is nearly identical to that of the tyrosyl radical. In summary, we have demonstrated the photoinitiated oxidation of tyrosine and tryptophan amino acids by observing both the one-electron-reduced and -oxidized quenching products.

Having verified that certain amino acid residues are potential oxidative damage targets within proteins, steady-state photolyses of each 1,8-naphthalimide derivative in the presence of lysozyme were carried out. 50 μM solutions of NI-ala, NI-tyr, and NI-trp were irradiated in the presence of 80 μM lysozyme. Aliquots were removed every hour up to 3 h to study the dependence of irradiation time on protein modification. Dark controls were done to ensure that the protein is intact without and with naphthalimide. The photoinduced products were separated by gel electrophoresis and visualized by poststaining with coomassie blue (see Supporting Information for the gel images). In the case of NI-ala, lysozyme modification was clearly observed during the first hour of exposure. Cleavage of lysozyme in the presence of NI-ala resulted in cleavage fragments in the 14−6.5 kDa range. At later irradiation times, the fading of the 14 kDa band indicates further, nonspecific cleavage of lysozyme. In addition to cleavage products, a higher molecular weight protein at ca. 27 kDa is also observed. Since the molecular weight of this protein is approximately twice that

of lysozyme, we attribute this band to cross-linked lysozyme induced by the NI-ala electronically excited states.

In the case of NI-tyr, protein modification is not observed until longer irradiation times are used. However, after 2−3 h of irradiation, fragmentation and cross-linking are clearly observed in the absence of "nonspecific" degradation. Similar results are observed when NI-trp is used as the photosensitizer.

Discussion

Previous reports have indicated that the presence of aromatic functional groups on organic photosensitizers facilitates noncovalent interactions with both BSA and lysozyme.[5,7] For the 1,8-naphthalimide derivatives used in this work, there is no evidence of ground-state interactions of either compound with the native proteins. Shifts in the UV absorption spectrum are not observed with the addition of protein. Furthermore, if such noncovalent interactions were present, curvature in the Stern−Volmer plots would be observed.

Redox Reactivity of Singlet NI-ala with Amino Acids and Proteins. From the results presented above, it is clear that both the singlet and triplet excited state of NI-ala are quenched by tyrosine, tryptophan, and the native proteins BSA and lysozyme. Quenching is not observed using nonaromatic amino acids or phenylalanine. The rate constants for singlet-state quenching by tryptophan and tyrosine are consistent with a diffusion-controlled bimolecular reaction. However, the rate constant of ca. 10^{10} M^{-1} s^{-1} measured for singlet-state quenching by tryptophan is nearly an order of magnitude higher than predicted for a diffusional reaction We considered the possibility of very weak π or electrostatic interactions between tryptophan and NI-ala leading to partial static quenching. However, there is no indication of strong intermolecular interaction from either the UV spectra or Stern−Volmer plots. Alternatively, the compound may interact with hydrogen donors through hydrogen-bonding interactions. Since these interactions take place remote to the π system, perturbations in the UV spectrum will be weak or nonexistent. To test this possibility, the singlet-state quenchings of NI-ala by tryptophan and *N*-methylindole were compared. Both compounds possess very similar oxidation potentials.[42] However, in *N*-methylindole, the hydrogen donor site on the indole ring is blocked. When *N*-methylindole was added to a 10 μM solution of NI-ala at a concentration of up to 9 mM, no fluorescence quenching was observed. Conversely, a ca. 25% reduction in fluorescence intensity is observed when only 5 mM of tryptophan is used. This result is consistent with the hypothesis that NI-ala and tryptophan are associated in the ground state via hydrogen-bonding interactions.

The redox properties of 1,8-naphthalimide derivatives as well as tyrosine and tryptophan have been reported. Using the one-electron reduction potential of NI ($E_{1/2}(\mathrm{NI/NI^{\bullet -}}) = -1.01$ vs NHE)[33] along with those of the amino acid radical cations ($E_{1/2}(\mathrm{TyrH^{\bullet +}/Tyr}) = 0.94$ and $E_{1/2}(\mathrm{TrpH^{\bullet +}/Trp}) = 1.05$ vs NHE at pH 7.0),[43] the thermodynamic driving force for electron transfer from these amino acids to the singlet excited state of NI is estimated from eq 4.

$$\Delta G = -[E_{1/2}(\mathrm{NI/NI^{\bullet -}}) - E_{1/2}(\mathrm{A^{\bullet +}/A})] - E_{^1\mathrm{NI}^*} \quad (4)$$

In eq 4, $E_{^1\mathrm{NI}^*}$ is the 0−0 excitation energy of the NI-ala singlet excited state (3.35 eV) and the reduction potentials are given above. From eq 4, electron transfer from either tryptophan or tyrosine to ^{1}NI* is exergonic by 1.29 and 1.4 eV, respectively. Thus, we attribute the singlet-state quenching to photoinduced electron transfer from these side chains.

When BSA is used as a quencher of the NI singlet excited state, the observed rate constant is ca. 500 times or 1600 times faster those that for tryptophan or tyrosine quenching, respectively. BSA is a 66 267 Da protein containing 2 tryptophans, 19 tyrosines, 17 histidines, and 59 lysines. Of these, only tryptophan, tyrosine, and histidine have been shown to quench ^{1}NI* in aqueous solution. While the structure of BSA is not known, it is certainly unlikely that all of these 38 quenching residues are near the protein surface and available to quench the naphthalimide singlet excited state. Even if it were the case, the bimolecular rate constant for singlet-state quenching by BSA is still more than 1 order of magnitude higher than one would expect if these residues in BSA were collectively quenched. Although the amine side chain of surface exposed lysine will exist in its protonated form at pH 7, those buried within the hydrophobic protein are likely to be in their free-base form. Free amines, for example DABCO, have been shown to effectively quench both the singlet and triplet excited state of 1,8-naphthalimide derivatives. Thus, we propose that the unusually large rate constant for the quenching of ^{1}NI* by BSA may be attributed to either (i) amino acid residues that will effectively quench ^{1}NI* when in a hydrophobic environment or (ii) weak, static interactions of NI with BSA that do not give rise to observable changes in the UV spectrum.

Likewise, the bimolecular rate constant for quenching by lysozyme is ca. 20 times or 65 times faster those that for tryptophan or tyrosine quenching, respectively. The structure of lysozyme has been reported.[44] The ∼14.7 kDa protein contains 6 tryptophans, 3 tyrosines, and 1 histidine. Again, considering only the possibility of quenching ^{1}NI* by these three amino acids, only 10 quenching residues are present per lysozyme. Thus, additional quenching from amino acids in the lysozyme hydrophobic interior (e.g., lysines in their basic form) or weak complexation is contributing to the very large bimolecular quenching constant.

Specifically, the sequence of lysozyme shows that a single histidine (His-15) is present beside an arginine (Arg-14) residue.[44] The presence of the Arg residue on the surface of lysozyme has been shown to attract negatively charged groups, such as carboxylic acids, toward this positively charged residue.[45] Therefore, electrostatic attraction of the carboxylic acid moiety of the naphthalimide chromophore toward this cavity, bringing it within "static" quenching distance of His-15, may be the cause of the unusually high singlet quenching constant of NI-ala by lysozyme. Work is ongoing to assess the naphthalimide−protein ground-state interactions.

Quenching of the singlet excited state of NI-ala by amino acids or proteins has relevance to oxidative damage mechanisms only if long-lived redox products are observed. In this context, we carried out laser flash photolysis experiments under conditions where the ^{1}NI-ala* was substantially quenched by either the free amino acids or native proteins. Immediately after the 355 nm excitation pulse, the spectrum looked identical to that of the NI triplet state, albeit substantially smaller due to the reduced intersystem crossing yield following singlet-state quenching. In summary, the oxidizable amino acids, as well as native proteins, do efficiently quench the singlet state of 1,8-naphthalimides. However, because of efficient charge recombination, redox products are not observed by laser flash photolysis. The result suggests that singlet-state quenching will not be the dominant oxidative damage route in proteins. In fact, this deactivation pathway is actually an energy-wasting pathway, since quenching occurs and long-lived products, either redox or triplet states, are not produced.

SCHEME 1: Kinetics of Triplet-Mediated Protein Oxidation and Proton-Coupled Charge Recombination

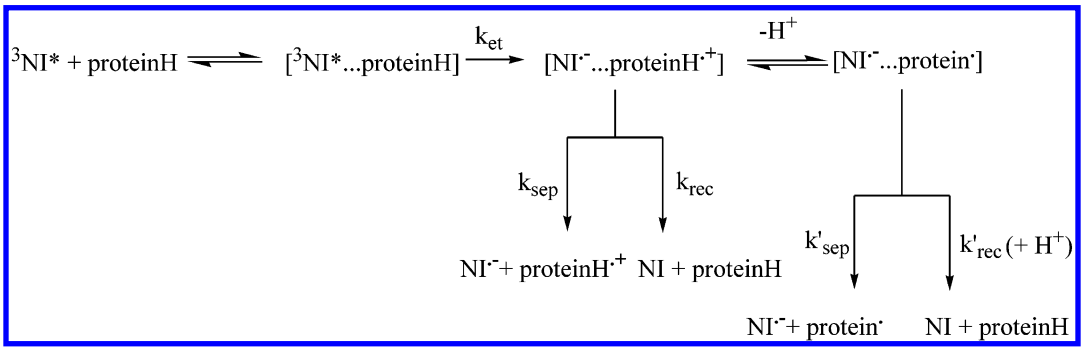

Redox Reactivity of Triplet NI with Amino Acids and Proteins. From Figures 3 and 5, it is apparent that tyrosine and tryptophan, but not histidine, also quench the NI-ala triplet state. Using an excitation energy of ^{3}NI* of 2.29 eV, along with eq 4, the thermodynamic driving forces for these reactions are estimated to be −0.34 and −0.23 eV for tyrosine and tryptophan, respectively. Unlike the singlet excited state, electron transfer to the NI-ala triplet from histidine does not occur. From Figure 3, it is apparent that long-lived redox products are formed following triplet-state quenching. The efficiency of radical production was quantified using benzophenone actinometry and found to be quite substantial (up to ca. 50% for free tryptophan).

Upon one-electron oxidation of tryptophan and tyrosine, the pK_a of the amino acid side chain is substantially reduced. For example, the pK_a of tyrosine changes from ca. 10 to −2 upon oxidation.[46] Similarly, a pK_a 4.3 has been reported for the tryptophan radical cation.[40] Thus, at the experimental pH of 7.0 used herein, we anticipate rapid deprotonation of both radical cations to give rise to the neutral tyrosyl and tryptophan radical. The spectra shown in Figures 6 and 7, under conditions where NI$^{\bullet-}$ is eliminated by reaction with oxygen, are consistent with production of the Trp$^{\bullet}$ and Tyr$^{\bullet}$ neutral radicals. The pH-dependent oxidation potentials of tyrosine and tryptophan have been reported.[47] In the case of tryptophan, the radical stabilization is ca. 135 mV upon deprotonation and slightly higher in the case of tyrosine. On the basis of thermodynamic driving force alone, back electron transfer to the neutral radicals is still predicted to be exergonic. In a separate study, the bimolecular rate constants for oxidation of 4-methoxyphenol by the neutral and protonated tryptophan radicals were measured.[48] Reaction involving the neutral radical was found to be nearly 3 orders of magnitude slower than the analogous redox reaction using the protonated radical, even though both were predicted to occur on the basis of thermodynamic arguments. The authors attributed the slow rate constant for reduction of the neutral radical to a large and unfavorable reorganization entropy associated with the proton-coupled electron transfer. Thus, the respectable quantum efficiency of radical production from photoinduced electron transfer is likely facilitated by rapid deprotonation of the oxidized amino acids.

Among other reports of the photooxidation of tyrosine and tryptophan, the photosensitized oxidation of tryptophan and tyrosine has recently been reported.[49] As reported herein, the yield of redox products was quite high (ca. 70%). The bimolecular rate constants for oxidation of both amino acids by riboflavin (RF) and flavin adenine dinucleotide (FAD) triplet states were shown to be $(1-2) \times 10^9$ M^{-1} s^{-1}. These values are similar to those reported in Table 1 for oxidation by ^{3}NI-ala*. In both cases, the electron-transfer reactions are at or near the diffusion-controlled limit.

In the context of photoinduced oxidative damage to native proteins, it is interesting to compare and contrast the results using BSA and lysozyme as reductive quenchers. As shown in Figure 5 and Table 1, both proteins diffusionally quench ^{3}NI-ala*. The bimolecular rate constants are similar to those measured for the free amino acids. Surprisingly, charge separation is only observed in our nanosecond laser flash photolysis experiments when lysozyme is used as a quencher. The quantum efficiency of 23% is somewhat smaller than that measured for the free amino acids. However, radicals are clearly observed following triplet-state quenching by lysozyme.

By comparison with our studies using the individual amino acids, we attribute the quenching to oxidation of one or more amino acids in the proteins. Both tyrosine and tryptophan are expected to be effective reductants for the triplet excited state of the naphthalimide. In addition, solvent-protected lysine residues that exist in their deprotonated form will also quench the excited state. The differences in charge separation efficiency following triplet-mediated lysozyme and BSA oxidation may be attributed to differences in solvent exposure of the oxidized residue. In recent work, the factors governing charge separation from DNA photolyase to photoactivated flavin have been addressed.[50] In this work, the authors demonstrated that fast charge recombination in the flavin−protein complex is inhibited by tryptophan deprotonation. Stated differently, the rate of charge recombination is governed by reprotonation of the neutral tryptophan radical. Within the protein, the specific tryptophan that was oxidized was found to be governed by their relative solvent exposure.

Triplet-mediated protein oxidation and subsequent thermal reactions are depicted in Scheme 1. From the rate constants measured herein, we can propose that amino acid oxidation in both BSA and lysozyme will occur, regardless of the domain in which the oxidizable residue is in. However, from the work of Popovic et al., it is clear that charge separation is facilitated by deprotonation of the oxidized tryptophan or tyrosine residue ($k'_{sep} > k'_{rec}$ in Scheme 1). If deprotonation cannot occur, due to the location of the oxidized amino acid, charge recombination will dominate ($k_{rec} > k_{sep}$ in Scheme 1). If deprotonation of the oxidized amino acid residue is crucial to producing long-lived charge separation, it is reasonable that, relative to BSA, lysozyme may have more tryptophan and tyrosine residues solvent exposed. The structure of lysozyme is well-known.[44] In this protein, tyr-20 and tyr-22 are separated by an arginine and glycine and are clearly in the solvent exposed region. In addition, trp-62 and trp-63 are somewhat exposed and accessible to proton-accepting solvent molecules. The structure of BSA has not been solved. However, the albumins are well-known to associate with fatty acids and other hydrophobic molecules,

suggesting that the electron-donating tryptophans, in particular, are likely to be buried in hydrophobic and solvent inaccessible sites.[51]

Upon comparing the photomodification results of lysozyme, induced by NI-ala, NI-trp, and NI-tyr, it is evident that the NI-ala cleaves and cross-links lysozyme faster than NI-trp and NI-tyr. The cross-linked photoproducts are most likely due to one-electron oxidation, followed by deprotonation, to yield neutral tryptophan or tyrosyl radicals. From our laser flash photolysis studies using lysozyme, it is known that amino acid oxidation on lysozyme does, indeed, occur. The yield of photocleavage products obtained with NI-ala is higher than that obtained with NI-trp and NI-tyr. This is most likely due to the longer-lived electronically excited state of NI-ala relative to the tryptophan- or tyrosine-substituted derivatives. It was hoped that the covalent linkage of the naphthalimide electron acceptor to aromatic amino acid donors would facilitate rapid and efficient charge separation to generate reactive tyrosine or tryptophan radicals in the vicinity of the protein. As indicated by the substantially reduced fluorescence quantum yield, forward charge transfer is, indeed, very rapid. However, the close proximity of the oxidized amino acid side chain and reduced naphthalimide facilitates fast charge recombination, since no long-lived transients are observed by laser flash photolysis. Further experiments are in progress to assess and identify the specific reactive intermediates responsible for cross-linking and cleaving the protein and optimizing the efficiency of protein photomodification.

Conclusions

In summary, this initial report indicates that 1,8-naphthalimide derivatives have utility as photoactivated probes of protein structure. We have demonstrated that these compounds show selectivity toward oxidizable amino acids, including tryptophan, tyrosine, and histidine. The reaction kinetics have been elucidated and, using laser flash photolysis, photoproducts clearly identified. From transient spectroscopy, we have observed the one-electron-reduced form of NI-ala following quenching by the native protein, lysozyme. All three naphthalimide derivatives studied have been shown to both cleave and cross-link the protein. Further experiments are in progress to assess and identify the specific reactive intermediates responsible for cross-linking and cleaving the protein and optimizing the efficiency of protein photomodification.

Acknowledgment. This work was supported by NSF Grant CHE-9984874.

Supporting Information Available: Figure showing separation of protein photoproducts using gel electrophoresis. This material is available free of charge via the Internet at http://pubs.acs.org.

References and Notes

(1) Radzicka, A.; Wolfenden, R. *J. Am. Chem. Soc.* **1996**, *118*, 6105−6109.
(2) Ramachandran, K. L.; Witkop, B. *Methods Enzymol.* **1976**, *11*, 283.
(3) Kaminskaia, N. V.; Johnson, T. W.; Kostic, N. M. *J. Am. Chem. Soc.* **1999**, *121*, 8663−8664.
(4) Kaminskaia, N.; Kostic, N. *Inorg. Chem.* **2001**, *40*, 2368−2377.
(5) Buranaprapuk, A.; Kumar, C. V.; Jockusch, S.; Turro, N. J. *Tetrahedron* **2000**, *56*, 7019−7025.
(6) Kumar, C. V.; Buranaprapuk, A.; Sze, H. C. *Chem. Commun.* **2001**, 297−298.
(7) Kumar, C. V.; Buranaprapuk, A. *J. Am. Chem. Soc.* **1999**, *121*, 4262−4270.
(8) Kumar, C. V.; Buranaprapuk, A.; Opiteck, G. J.; Moyer, M. B.; Jockusch, S.; Turro, N. J. *Proc. Natl. Acad. Sci. U.S.A.* **1998**, *95*, 10361−10366.
(9) Gill, G.; Richter-Rusli, A. A.; Ghosh, M.; Burrows, C.; Rokita, S. E. *Chem. Res. Toxicol.* **1997**, *10*, 302−309.
(10) Brown, K. C.; Yu, Z.; Burlingame, A. L.; Craik, C. S. *Biochemistry* **1998**, *37*, 4397−4406.
(11) Person, M. D.; Brown, K. C.; Mahrus, S.; Craik, C. S.; Burlingame, A. L. *Protein Sci.* **2001**, *10*, 1549−1562.
(12) Amini, F.; Kodadek, T.; Brown, K. C. *Angew. Chem., Int. Ed.* **2002**, *41*, 356−359.
(13) Spikes, J. D.; Shen, H.-R.; Kopeckova, P.; Kopecek, J. *Photochem. Photobiol.* **1999**, *70*, 130−137.
(14) Kim, K.; Fancy, D. A.; Carney, D.; Kodadek, T. *J. Am. Chem. Soc.* **1999**, *121*, 11896−11897.
(15) Fancy, D. A.; Kodadek, T. *Proc. Natl. Acad. Sci. U.S.A.* **1999**, *96*, 6020−6024.
(16) Barry, B. A.; El-Deeb, M. K.; Sandusky, P. O.; Babcock, G. *J. Biol. Chem.* **1990**, *265*, 20139−20143.
(17) Karthein, R.; Dietz, R.; Nastainczyk, W.; Ruf, H. H. *Eur. J. Biochem.* **1988**, *171*, 313−320.
(18) Huyett, J. E.; Doan, P. E.; Gurbiel, R.; Housemann, A. L. P.; Sivaraja, M.; Goodin, D. B.; Hoffman, B. M. *J. Am. Chem. Soc.* **1995**, *117*, 9033−9041.
(19) Wagenknecht, H.-A.; Stemp, E. D. A.; Barton, J. K. *Biochemistry* **2000**, *39*, 5483−5491.
(20) Brana, M. F.; Dominguez, G.; Saez, B.; Romerdahl, C.; Robinson, S.; Barlozzari, T. *Eur. J. Med. Chem.* **2002**, *37*, 541−551.
(21) Brana, M. F.; Castellano, J. M.; Moran, M.; Perez de Vega, M. J.; Perron, D.; Conlon, D.; Bousquet, P. F.; Romerdahl, C. A.; Robinson, S. P. *Anti-Cancer Drug Des.* **1996**, 297−309.
(22) Brana, M. F.; Castellano, J. M.; Roldan, C. M.; Vazquez, D.; Jiminez, A. *Cancer Chemother. Pharmacol.* **1980**, *4*, 61−66.
(23) Brana, M. F.; Sanz, A. M.; Castellano, J. M.; Roldan, M. C.; Roldan, C. *Eur. J. Med. Chem.* **1981**, *16*, 207−212.
(24) Matsugo, S.; Kawanishi, S.; Yamamoto, K.; Sugiyama, H.; Matsuura, T.; Saito, I. *Angew. Chem., Int. Ed. Engl.* **1991**, *30*, 1351−1353.
(25) Saito, I.; Takayama, M. *J. Am. Chem. Soc.* **1995**, *117*, 5590−5591.
(26) Saito, I.; Takayama, M.; Sugiyama, H.; Nakatani, K. *J. Am. Chem. Soc.* **1995**, *117*, 6406−6407.
(27) Aveline, B. A.; Matsugo, S.; Redmond, R. W. *J. Am. Chem. Soc.* **1997**, *119*, 11785−11795.
(28) Rogers, J. E.; Weiss, S. J.; Kelly, L. A. *J. Am. Chem. Soc.* **2000**, *122*, 427−436.
(29) Zhang, J.; Woods, R. J.; Brown, P. B.; Lee, K. D.; Kane, R. R. *Bioorg. Med. Chem. Lett.* **2002**, *12*, 853−856.
(30) Yamamoto, T.; Meaeda, Y.; Matsugo, S.; Kitano, H. *Photochem. Photobiol.* **1997**, *66*, 65−71.
(31) Rogers, J. E.; Abraham, B.; Rostkowski, A.; Kelly, L. A. *Photochem. Photobiol.* **2001**, *74*, 521−531.
(32) Pace, C. N.; Vajdos, F.; Fee, L.; Grimsley, G.; Gray, T. *Protein Sci.* **1995**, *4*, 2411−2423.
(33) Rogers, J. E.; Kelly, L. A. *J. Am. Chem. Soc.* **1999**, *121*, 3854−3861.
(34) Carmicheal, I.; Hug, G. L. *J. Phys. Chem. Ref. Data* **1986**, *15*, 54.
(35) Barros, T.; Molinari, G. R.; Filho, P. B.; Toscano, V. G.; Politi, M. J. *J. Photochem. Photobiol. A* **1993**, *76*, 55−60.
(36) Poliakov, P.; Arnold, B. A. *Spectrosc. Lett.* **1999**, *32*, 747−762.
(37) Rogers, J. E.; Le, T. P.; Kelly, L. A. *Photochem. Photobiol.* **2001**, *73*, 223−229.
(38) Bensasson, R. V.; Land, E. J.; Truscott, T. G. *Flash Photolysis and Pulse Radiolysis: Contributions to the Chemistry of Biology and Medicine*; Pergamon: New York, 1983; pp 105−108.
(39) Lynn, K. R.; Purdie, J. W. *Int. J. Radiat. Phys. Chem.* **1976**, *8*, 685−689.
(40) Posener, M. L.; Adams, G. E.; Wardman, P.; Cundall, R. B. *J. Chem. Soc., Faraday Trans. 1* **1976**, *72*, 2231−2239.
(41) Solar, S.; Getoff, G.; Surdhar, P. S.; Armstrong, D. A.; Singh, A. *J. Phys. Chem.* **1991**, *95*, 3636−3643.
(42) Merenyi, G.; Lind, J.; Shen, X. *J. Phys. Chem.* **1988**, *92*, 134−137.
(43) DeFelippis, M. R.; Murthy, C. P.; Broitman, F.; Weinraub, D.; Faraggi, M.; Klapper, M. H. *J. Phys. Chem.* **1991**, *95*, 3416−3419.
(44) Blake, C. C. F.; Koenig, D. F.; Mair, G. A.; North, C. T.; Phillips, C. D.; Sarma, V. R. *Nature (London)* **1965**, *206*, 757−761.
(45) Yamada, H.; Uozumi, F.; Ishikawa, A.; Imoto, T. *J. Biochem.* **1984**, *95*, 503−550.
(46) Land, E. J.; Porter, G.; Fang, J. Y.; Strachan, E. *Trans. Faraday Soc.* **1961**, *57*, 1885−1893.
(47) Harriman, A. *J. Phys. Chem.* **1987**, *91*, 6102−6104.
(48) Jovanovic, S. V.; Steenken, S.; Simic, M. *J. Phys. Chem.* **1991**, *95*, 684−687.
(49) Lu, C.-Y.; Liu, Y.-Y. *Biochim. Biophys. Acta* **2002**, *1571*, 71−76.
(50) Popovic, D. M.; Zmiric, A.; Aaric, S. D.; Knapp, E.-W. *J. Am. Chem. Soc.* **2002**, *124*, 3775−3782.
(51) He, X. M.; Carter, D. C. *Nature (London)* **1992**, *358*, 209−215.